DALTON
FULL PAPER

An electrospray ionization mass spectrometry study of the nitroprusside–cation–thiolate system

Geoffrey A. Lawrance,*[a] Marcel Maeder,[a] Yorck-Michael Neuhold,[a] Konrad Szaciłowski,[b] Andrea Barbieri[c] and Zofia Stasicka*[b]

[a] *Discipline of Chemistry, School of Environmental and Life Sciences, The University of Newcastle, Callaghan 2308, Australia*
[b] *Faculty of Chemistry, Jagiellonian University, Ingardena 3, 30-060 Kraków, Poland*
[c] *Department of Chemistry, University of Ferrara, Via Borsari 46, 44100 Ferrara, Italy*

Received 7th June 2002, Accepted 20th August 2002
First published as an Advance Article on the web 4th September 2002

The complex anion $[Fe(CN)_5(NO)]^{2-}$ (nitroprusside) has been defined intact using electrospray ionization mass spectrometry (ESIMS), with minor daughter ions predictable fragments of the parent $[Fe(CN)_5NO]^{2-}$. Direct evidence for ion pairing of $[Fe(CN)_5NO]^{2-}$ with monovalent alkali metal and some alkylammonium cations was found independently using ESIMS and ^{13}C NMR techniques. The results are relevant to the significant influence of the concentration and nature of cations on the solution equilibrium between nitroprusside with thiolates and their nitrosothiol adducts that presumably arises through charge reduction in tight ion pairs facilitating adduct formation. Ion-paired species $\{M^+[Fe(CN)_5NO]^{2-}\}^-$, $\{M_3[Fe(CN)_5NO]\}^+$ and more complex clusters of the type $\{M_x[Fe(CN)_5NO]_y\}^{z-/z+}$ (up to $x = 8$ and $y = 5$) were observed by ESIMS. The trend in the ion pair formation seen by ESIMS follows the series $Li^+ > Na^+ > K^+ > Rb^+ > Cs^+$ and $Me_4N^+ > Et_4N^+ > Pr_4N^+ > Bu_4N^+$ and is consistent with purely electrostatic expectations for unsolvated ions. Whereas the poorly solvated alkylammonium series bulk solution behaviour resembles that found by the ESI technique, the activity of alkali metal cations proceeds conversely, *i.e.* $Li^+ < Na^+ < K^+ < Rb^+ < Cs^+$, verified by a ^{13}C NMR study, because the hydrated cation radii play a crucial role in the bulk solution in those cases. Differences in changes of the chemical shift upon addition of various cations points to the axial CN^- position as especially important for binding to these cations. Further, short-lived adducts with thiolates of the type $\{M^+_3[Fe(CN)_5NO(C_4H_4O_4S)]^{4-}\}^-$ have been defined by their observation in ESIMS directly and through their decomposition products, providing further support for reversible nitrosothiol complex formation. Mercaptosuccinate ion pairing with cations, which would make formation of the proposed nitrosothiol complex easier, is also observed by ESIMS. The dithiolato complex $\{K^+[Fe(CN)_5NO(C_4H_6O_4S)_2]^{2-}\}^-$, as well as the disulfide anion radical were detected; both species are suggested intermediates in the spontaneous and autocatalyzed redox decomposition of the $[Fe(CN)_5N(O)SR]^{(n+2)-}$ complexes. The ESIMS study has thus provided information relevant to both thermodynamic and kinetic processes in a reaction where species of limited stability are involved.

Introduction

Due to free electron pairs localized on the N-atoms of the CN^- ligands, transition metal cyanide complexes are known for their marked susceptibility towards interaction with the medium. Consequently, their thermal and photochemical reactivities are modulated by medium factors (*e.g.* solvent, pressure, ionic strength, nature of cations).[1–19] To the most intensively studied systems belong penta- and hexa-cyanoferrates(II) and (III), for which not only reactivity but also spectroscopic properties are influenced by these factors. In particular, energies of the CT transitions (MLCT in Fe(II), and LMCT in the Fe(III) complexes) undergo bathochromic and hypsochromic shifts, respectively, when the solvent polarity is increased.[7–12] The shifts were found to be proportional to the acceptor number of the solvent, and interpreted in terms of specific solvent interaction with the free *N*-localized electron pairs.[7–12]

Similar interactions are responsible for the specific cation effect in diverse cyanocomplexes. Hexacyanoferrates(II) and (III) are known to form weak ion-pairs with alkali metal ions: the stability constants vary with ion, from 0.48 to 3.3 for sodium and caesium cations, respectively.[13–15] Electron transfer between the Fe(II) and Fe(III) complexes is enhanced by the ion-pair formation with inorganic cations (in the order $Cs^+ > K^+ > NH_4^+ > Li^+$), whereas the opposite effect is observed in the presence of tetraalkylammonium cations (the ET rate decreases in the order: methyl > ethyl > butyl).[16–18] The tendency, observed for inorganic cations, consistent with the desolvation order, was interpreted in terms of formation of the $\{[Fe(CN)_6]^{3-}\ldots M^+\ldots[Fe(CN)_6]^{4-}\}$ aggregates.[16–18] Similar behaviour was observed in reaction between hexacyanoferrate(III) and other reducing agents.[5,19]

Beside electron transfer processes, the ion-pair formation influences the substitution reactions: the specific complex–electrolyte and ligand–electrolyte interactions can lead both to an increase and decrease of the substitution rate.[7–9] Interaction of inorganic cations with the free electron pairs of the CN^- ligands in the $[Fe(CN)_5L]^{n-}$ complexes decreases the negative charge on the central ion and thereby the Fe–L bond becomes strengthened (when L = σ-donor ligand) or weakened (for L = σ-donor + π-acceptor). The effect is sensitive to the polarity of the medium and hence the opposite influence of the tetraalkylammonium cations is observed.[7–9]

One of the most intensively studied $[Fe(CN)_5L]^{n-}$ complexes is the nitrosylpentacyanoferrate(II) ion, commonly called nitroprusside (NP). The interest follows recent developments in phototherapy pertaining to NO delivery to selected tissues.[20–26] This aspect has stimulated the search for compounds that are able to behave as the NO-carriers. Sodium nitroprusside itself is a widely used nitrovasodilator, but the detailed mechanism of

Table 1 Negative-ion ESI-MS results for 2×10^{-4} M $Na_2[Fe(CN)_5(NO)]$ in aqueous solution under different cone voltages (CV) [a]

Species	m/z_{theor}	m/z_{obs}	%BPI (10 V)	%BPI (20 V)	%BPI (40 V)	%BPI (60 V)
CN^-	26	26.0	<0.1	0.6	4.8	15.4
$[Fe(CN)_5]^{2-}$	93	92.7	49	52	<0.1	<0.1
$[Fe(CN)_5NO]^{2-}$	108	107.8	100	48	100	100
$[Fe(CN)_3]^-$	134	133.6	5.1	100	81	15
$[Fe(CN)_2NO]^-$	138	137.6	0.5	5.8	16	5.1
$[Fe(CN)_4]^-$	160	159.8	0.5	33	10	1.9
$[Fe(CN)_3NO]^-$	164	163.6	1.6	2.3	<0.1	<0.1
$\{H^+[Fe(CN)_5]^{2-}\}^-$	187	186.6	<0.1	3.2	2.6	1.0
$[Fe(CN)_4NO]^-$	190	189.9	0.1	0.3	<0.1	<0.1
$[Fe(CN)_4(NO)(H_2O)]^-$	208	208.8	<0.1	2.6	4.5	0.6
$\{H^+[Fe(CN)_5NO]^{2-}\}^-$	217	216.8	2.9 (2.8) [b]	3.5	<0.1	<0.1
$\{Na^+[Fe(CN)_5NO]^{2-}\}^-$	239	238.8	7.0 (10.7) [b]	21.0	2.4	1.3
$\{Na_4[Fe(CN)_5NO]_3\}^{2-}$ [c]	370	369.9	0.2	0.6	0.2	<0.1
$\{Na_3[Fe(CN)_5NO]_2\}^-$ [c]	501	500.7	<0.1	0.6	0.8	0.3
$\{Na_8[Fe(CN)_5NO]_5\}^{2-}$ [c]	632	631.9	<0.1	0.1	<0.1	<0.1
$\{Na_5[Fe(CN)_5NO]_3\}^-$ [c]	763	762.9	<0.1	0.2	0.6	0.6

[a] Cluster peaks are also observed in the positive ion ESIMS, *e.g.* $\{Na_3[Fe(CN)_5NO]\}^+$ at *m/z* 285.0 (theor. 285), $\{Na_3[Fe(CN)_5NO]\}^+ \cdot H_2O$ at 303.0 (theor. 303) and $\{Na_5[Fe(CN)_5NO]_2\}^+$ at *m/z* 547.0 (theor. 547). [b] With added sodium ion; 1 : 1 complex : NaOH. [c] Increase in relative intensity as complex concentration is increased.

its physiological action is still not fully understood. Also, different *S*-nitrosothiols, RSNO, have been studied as potential NO-donors.[24–26] They have been suggested to be effective against leukemic cells due to NO and $RS^{\bullet}$ generation.[24] It is known[27–34] that nitroprusside and thiolates generate *S*-nitrosothiol complexes in the reversible reaction (1).

$$[Fe(CN)_5NO]^{2-} + RS^{n-} \rightleftarrows [Fe(CN)_5N(O)SR]^{(n+2)-} \quad (1)$$

In most cases the reaction product is thermally unstable and in redox decomposition yields a Fe(II) complex and a disulfide,[27–34]

$$[Fe(CN)_5N(O)SR]^{(n+2)-} \longrightarrow [Fe^{II}(CN)_5NO]^{3-} + \tfrac{1}{2}RSSR \quad (2)$$

Previous studies[29–30] showed that cations play a crucial role in shifting the equilibrium between nitroprusside, thiolate and nitrosothiol complex [eqn. (1)]. Small alkali metal cations promote $[Fe(CN)_5N(O)SR]^{3-}$ formation, whereas bulky cations (*e.g.* tetrabutylammonium) retard the complex formation. The shift was used to evaluate the ion-pair formation constant.[29]

Recently it was found, that not only the thermal behaviour of the $[Fe(CN)_5N(O)SR]^{3-}$ complex, but also its photochemical reactivity is cation-dependent. As the dependence is quantitative, not qualitative, the quantum yield values could also be used to estimate the cation effectiveness in the ion-pair formation between the $[Fe(CN)_5NO]^{2-}$ complex and a specific cation.[35,36] In seeking further evidence to verify the conclusions, the ESIMS technique, which is useful in demonstrating the presence of the charged chemical species resulting from ion–ion and ion–molecule associations in solution, has been applied.

The identification of complex ions by ESIMS and understanding of their behaviour under ESI conditions has been attracting attention recently. The relatively 'soft' technique of ESIMS permits identification of even labile complex ions in an intact form, and appears to reflect speciation in bulk solution.[37–40] Further, the ability to capture, through the use of ESIMS, information relating to kinetic and thermodynamic processes in the bulk solution has been recognised.[41] Although complex cations have been the subject of a number of studies, complex anions have attracted relatively little attention to date, apart from polyoxometallates[42] and some metal complexes with inorganic and/or organic ligands, mostly of biological importance.[43] Among others, the electrospray method has been used successfully to investigate some cyanide complexes ($[Ru^{II}L_2(CN)_2]$)[44,45] and iron or ruthenium nitrosyl complexes ([Fe(NO)(haemoglobin)], [Fe(NO)(TPP)],[46] $[Fe_7S_4(NO)_8]^-$, $[Fe_7S_6(NO)_{10}]^-$,[47] $[Ru(NO)Cl_2(imH)_2(H_2O)]^+$,[48] and $[RuCl_3(NO)(PPh_3)_2]$[49]). Here, because of our interest in its reactions, we examine the $[Fe(CN)_5NO]^{2-}$ complex ion, and some of its interactions.

Results and discussion

ESIMS spectrum of $Na_2[Fe(CN)_5NO]$ in aqueous solution

The integrity of the $[Fe(CN)_5NO]^{2-}$ complex ion is retained in large part in the negative ion ESIMS at low cone voltage, as illustrated in Fig. 1. The major peak (100% BPI) at *m/z* 107.8

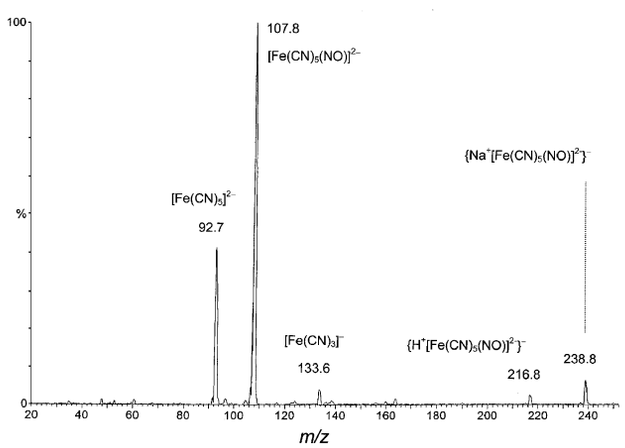

Fig. 1 ESIMS of a 1×10^{-4} M aqueous solution of $Na_2[Fe(CN)_5NO]$ at a CV of 10 V.

is assigned as $[Fe(CN)_5NO]^{2-}$ (theoretical *m/z* calculated for the major isotopes = 108). The only other major peak occurs at *m/z* 92.7, assigned to the oxidized Fe(III) nitrosyl-dissociated fragment $[Fe(CN)_5]^{2-}$ (theor. *m/z* = 93). A smaller peak at *m/z* 133.6 is consistent with a fragment $[Fe^{II}(CN)_3]^-$ (theor. *m/z* = 134) arising *via* loss of $(CN)_2^-$ from the pentacyano species. This signal could also arise from a cluster species $[Fe^{II}(CN)_3]_n^{m-}$; however, the presence of another smaller peak two mass units less with a relative intensity consistent with its assignment as the 5.8% abundant ^{54}Fe isotope complex, and a smaller shoulder one mass unit higher from the 2.2% abundant ^{57}Fe, supports the formulation as a simple monomer. Some other minor peaks arising from cyanide loss rather than nitrosyl loss occur and are tentatively assigned in Table 1, but appear more intense mainly at higher cone voltages; overall, fragmentation is not important at low cone voltage.

Other peaks observed arise, importantly, from ion-paired adducts; $\{H^+[Fe(CN)_5NO]^{2-}\}^-$ appears at *m/z* 216.8 (theor.

Table 2 ESIMS for 2×10^{-4} M $Na_2[Fe(CN)_5NO]$ in the presence of equimolar concentrations of MCl with respect to Na^+, at a CV of 10 V

M^+	Species	m/z_{theor}	m/z_{obs}	%BPI
Li^+	$Li(H_2O)_2^+$	43	42.9	22
	$Li(H_2O)_3^+$	61	60.9	15
	$\{Li^+[Fe(CN)_5NO]^{2-}\}^-$	223	222.9	2.3 (2.3)[b]
Na^+	$Na(H_2O)^+$	41	40.9	13
	$Na(H_2O)_2^+$	59	58.8	16
	$\{Na^+[Fe(CN)_5NO]^{2-}\}^-$	239	238.9	2.3 (1.5)[b]
K^+	K^+	39	38.9	4.8
	$K(H_2O)^+$	57	56.8	36
	$K(H_2O)_2^+$	75.1	74.8	2.1
	$\{K^+[Fe(CN)_5NO]^{2-}\}^-$	255	254.9	1.6 (0.8)[b]
Rb^+	Rb^+	85; 87	84.7; 86.7	27; 6.9
	$Rb(H_2O)^+$	103; 105	102.7; 104.7	59; 23
	$Rb(H_2O)_2^+$	121; 123	120.7; 122.8	1.5; 0.6
	$[Rb_2(H_2O)(H_2CO_3)]^{2+}$ [a]	125; 127	125.7; 127.7	35; 14
	$[Rb_2(HCO_3)]^+$ [a]	231; 233	230.8; 232.8	2.5; 1.9
	$\{Rb^+[Fe(CN)_5NO]^{2-}\}^-$	301; 303	300.9; 302.9	2.0; 0.6 (0.5)[b]
Cs^+	Cs^+	133	132.7	66
	$Cs(H_2O)^+$	151	150.8	100
	$[Cs_2(H_2O)(H_2CO_3)]^{2+}$ [a]	173	173.9	7.9
	$[Cs_2(HCO_3)]^+$ [a]	327	327.0	4.9
	$\{Cs^+[Fe(CN)_5NO]^{2-}\}^-$	349	348.9	2.5 (0.3)[b]

[a] 50-Fold excess of M^+ (M_2CO_3). [b] Adjusted for ion efficiency by calibration against the corresponding equimolar $Li^+/Na^+/K^+/Rb^+/Cs^+$ free ion spectra; $\{Rb^+[Fe(CN)_5NO]^{2-}\}^-$ was calibrated to the sum of the Rb^+ isotope peaks; all negative ion %BPI are relative to the 100% BPI of $[Fe(CN)_5NO]^{2-}$ at *m/z* 107.8.

m/z = 217) and $\{Na^+[Fe(CN)_5NO]^{2-}\}^-$ at *m/z* 238.8 (theor. *m/z* = 239). Apart from these ions, some very low intensity signals are seen at higher *m/z* values, which can be assigned to more complex clusters of the general type $\{Na_x[Fe(CN)_5NO]_y\}^{z-}$. Members of a series with up to $x = 8$ and $y = 5$ are detected, and are defined in Table 1. Members of the family with $x = y$ would have the same *m/z* as that assigned to the $\{Na^+[Fe(CN)_5NO]^{2-}\}^-$ species ($x = y = 1$). However, they are anticipated to be very minor species by analogy with those where $x \neq y$. This is confirmed by the isotopic Fe pattern observed, which defines the 1 : 1 adduct as very dominant. Although the clusters increase in intensity with increasing concentration of nitroprusside, the intensities relative to the major peaks always remain very small. The observation of ion-paired series has been reported before, for the family $[M_{2m-2}W_mO_{4m}]^{2-}$ (M = Li, Na, K) for *m* values from 1 up to 11,[42] although in that case polymerization is involved.

The effect of cone voltage on the ESIMS is reasonably significant, although the $[Fe(CN)_5NO]^{2-}$ complex ion remains the major or a dominant peak. The behaviour as CV is increased is consistent with increasing dissociation, as reflected in a consistent increase in the size of a peak due to cyanide ion at *m/z* 26 with increasing CV, although trends amongst peaks are not simple. For example, the peak at *m/z* 133.6 assigned to $[Fe^{II}(CN)_3]^-$ increases significantly in size from CV 10 to 20 V, but falls substantially again by 60 V. The growth and fall of this peak is matched by a lower intensity one at *m/z* 159.8, assigned to a related $[Fe^{III}(CN)_4]^-$ species. Species observed at different CV values are collected and assigned in Table 1.

As the concentration of complex is increased in the ESIMS experiment from 1×10^{-4} through to 1×10^{-3} M, the relative intensities of the various peaks vary in different ways. The parent ion relative signal decreases with concentration, which can be interpreted as arising from a greater potential to undergo collisions and hence undergo collision-enhanced dissociation as the concentration rises. The concentration of the sodium ion-paired adducts rises with increasing overall concentration, presumably related to an increase in the probability of ion encounter and subsequent ion pair formation. There is also a rise in the amount of minor high *m/z* presumed cluster species, again anticipated as encounter probability is enhanced. Relatively constant intensity for the putative $[Fe^{II}(CN)_3]^-$ species is more consistent with it being monomeric, as assigned, rather than a cluster species. However, the concentration dependencies seen are far less significant than the influence of CV, as anticipated, and the overall pattern of peaks remains. From this initial study it is apparent that low CV and low concentration produce quite 'clean' spectra dominated by the $[Fe(CN)_5NO]^{2-}$ complex ion. Further, evidence of ion-paired species is forthcoming. The $\{Na_3^+[Fe(CN)_5NO]^{2-}\}^+$ adduct occurs as a 7.0% BPI (*i.e.* relative to the base peak intensity) peak in the solution of the complex in water alone. Addition of an equimolar amount of NaOH leads to an enhanced signal (to 10.7% BPI), as expected from the increased concentration of sodium ion present. Thus, not only the ion pairing is observed, but also the ESIMS outcome appears to reflect anticipated bulk solution properties. This is pursued further below.

The positive ion ESIMS of $Na_2[Fe(CN)_5NO]$ has no high intensity peaks apart from $Na(OH_2)_n^+$ species; otherwise, it is dominated by a peak due to $[FeOH]^+$ (m/z_{obsd} 63.8, m/z_{theor} 65), resulting from dissociations which also release cyanide (found in the negative ion spectrum). Some very minor peaks associated with $[FeCN]^+$ (*m/z* 81.8; 82), $[Fe(CN)_2]^+$ (*m/z* 106.7; 108), $[Fe_2(O)(OH)]^+$ (*m/z* 128.9; 129), $\{Na_3[Fe(CN)_5NO]\}^+$ (*m/z* 285.0; 285) and $\{Na_5[Fe(CN)_5NO]_2\}^+$ (*m/z* 547.0; 547) were also observed. Further, the observation of a smaller peak due to the solvated species $\{Na_3[Fe(CN)_5NO]\}^+ \cdot H_2O$ (*m/z* 303.0; 303) is noted, and supports the cluster formulation assigned. The formation of ion-paired cationic species, albeit in relatively small amounts, is notable, and fits the appearance of a general series of ion paired $\{Na_x[Fe(CN)_5NO]_y\}^{z-/z+}$ species at least for the low charged ($z = 1$ or 2) species favoured in ESIMS.

Ion pairing investigations

(i) ESIMS method. The observation above of ion pairs for $[Fe(CN)_5NO]^{2-}$ with H^+, Na^+ and K^+ led to a fuller analysis of ion pair formation with this complex anion (Table 2). The capacity to form ion pairs is clearly illustrated in Fig. 2, where 1 : 1 ion pairs are observed for all alkali metal ions when equimolar concentrations of each and the complex anion are present in solution. The apparent peak intensities are not a direct reflection of relative concentrations, since ionization efficiency varies with ion size. After adjusting the observed data for the intensity enhancement with increasing cation mass (*via* calibration against solutions of the corresponding

Table 3 ESIMS for 2×10^{-4} M $Na_2[Fe(CN)_5NO]$ in the presence of equimolar concentrations of RCl with respect to Na^+, at a CV of 10 V

R^+	Species	m/z_{theor}	m/z_{obs}	%BPI
Me_4N^+	Me_4N^+	74	73.9	5.7
	$Me_4N^+ \cdot Me_4NCl$ [a]	183; 185	183.1; 185.1	12; 3.7
	$Me_4N^+ \cdot Bu_4NCl$	351; 353	351.4; 353.3	0.1;0.05
	$Me_4NCl_2^-$	144; 146	143.8; 145.8	0.4; 0.2
	$(Me_4NCl)_2Cl^-$ [a]	253; 255	253.1; 255.1	1.8; 1.7
	$\{[(Me_4N)^+[Fe(CN)_5NO]^{2-}\}^-$	290	290.0	0.5 (0.5) [b]
	$\{[(Me_4N)^+[Fe(CN)_5NO]^{2-}\}^- \cdot Me_4NCl$ [a]	399; 401	399.2; 401.3	0.7; 0.2
Et_4N^+	Et_4N^+	130	130.0	32
	$Et_4N^+ \cdot Bu_4NCl$	407; 409	407.6; 409.5	0.44;0.1
	$Et_4NCl_2^-$	200; 202	199.9; 202.1	0.5; 0.3
	$\{[(Et_4N)^+[Fe(CN)_5NO]^{2-}\}^-$	346	346.2	0.7 (0.11) [b]
Pr_4N^+	Pr_4N^+	186	186.1	100
	$Pr_4N^+ \cdot Bu_4NCl$	463; 465	463.6; 465.6	0.9; 0.3
	$\{[(Pr_4N)^+_3[Fe(CN)_5NO]^{2-}\}^+$	774	774.8	0.05
	$Pr_4NCl_2^-$	256; 258	256.1; 258.1	1.1; 0.7
	$\{[(Pr_4N)^+[Fe(CN)_5NO]^{2-}\}^-$	402	402.3	1.9 (0.09) [b]
Bu_4N^+	Bu_4N^+	242	242.3	98
	$Bu_4N^+ \cdot Bu_4NCl$	519; 521	519.7; 521.6	0.8; 0.3
	$\{[(Bu_4N)^+_3[Fe(CN)_5NO]^{2-}\}^+$	942	943.2	0.08
	$\{[(Bu_4N)^+_2(Pr_4N)^+[Fe(CN)_5NO]^{2-}\}^+$	886	886.9	0.08
	$\{[(Bu_4N)^+(Pr_4N)^+_2[Fe(CN)_5NO]^{2-}\}^+$	830	830.4	0.05
	$Bu_4NCl_2^-$	312; 314	312.2; 314.2	1.1; 0.7
	$\{[(Bu_4N)^+[Fe(CN)_5NO]^{2-}\}^-$	458	458.3	3.1 (0.14) [b]

[a] 50-Fold excess of Me_4NCl. [b] Adjusted for ion efficiency by calibration against the corresponding equimolar $Me_4N^+/Et_4N^+/Pr_4N^+/Bu_4N^+$ free ion spectra; all negative ion %BPI are relative to the 100% BPI of $[Fe(CN)_5NO]^{2-}$ at m/z 107.8.

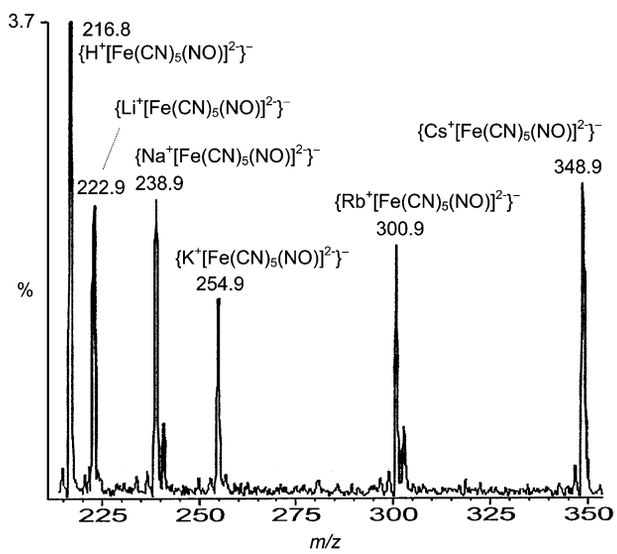

Fig. 2 Section of the ESIMS of a solution containing a 1 : 1 : 1 : 1 : 1 ratio of Li : Na : K : Rb : Cs ions with $[Fe(CN)_5NO]^{2-}$ ([anion] = 2×10^{-4} M; cation : complex 2 : 1) recorded at a cone voltage of 10 V, showing 1 : 1 ion paired species.

equimolecular free cation spectra) the trend in concentration profiles is, as anticipated, for lower amounts of ion paired species with increasing ion size (Table 2). This is consistent with pure electrostatic arguments for unsolvated ions. This observation is enhanced by an additional experiment, where increasing amounts of K_2CO_3 were added to a solution of $Na_2[Fe(CN)_5NO]$. The unadjusted relative intensities of the K^+/Na^+ ion paired peaks as the ratio was varied from 1 : 1 (a ratio of 0.46), to 5 : 1 (1.0), to 10 : 1 (4.3) and to 50 : 1 (36) reflect the anticipated significant increase in the K^+ ion pair in the bulk solution as the concentration of K^+ is raised. Similar experiments were carried out using Rb_2CO_3, Cs_2CO_3 and Me_4NCl.

Ion pairing was investigated and observed not only with the simple alkali ions Li^+, Na^+, K^+, Rb^+ and Cs^+ (Table 2), but also with the large organic ions Me_4N^+, Et_4N^+, Pr_4N^+ and Bu_4N^+ (Table 3). In each case there is an increase in the intensity of the ion pair signal as the ratio of cation to anion is increased (typically the range from 1 : 1 to 10 : 1 was examined), reflecting bulk solution behaviour. Further, allowing for variations in signal intensity with cation, the trend in the amount of ion pair formation is Li^+ (unsolvated ionic radius 68 pm) > Na^+ (97 pm) > K^+ (133 pm) > Rb^+ (147 pm) > Cs^+ (167 pm) and Me_4N^+ > Et_4N^+ > Pr_4N^+ > Bu_4N^+. This is fully consistent with the expectations based on purely electrostatic arguments, where unsolvated cations are present, as is the case in the ESIMS experiment. Further, the amount of ion-paired species at the applied nitroprusside and cations concentrations is low compared with the unassociated complex ion (<10% total). Since ion-pairing constants in water are low, this is anticipated. In fact, the amount of ion pairing seen in the ESIMS is almost certainly greater than that observed in solution, since the droplet drying process must introduce concentration effects that should influence the abundance, but less likely the relative ratios, of ion-paired species.[50] It would appear that the ESIMS results reflect the situation in the bulk precursor solutions somewhat, albeit exaggerated by subsequent processes in the ESI unit.

(ii) ^{13}C NMR observations. To verify the hypothesis, the cation effect on the ^{13}C NMR spectrum of nitroprusside was measured (Table 4). In aqueous solutions chemical shifts are equal to 132.5 and 134.65 ppm for axial and equatorial CN^- ligands, respectively (consistent with the previous report[51]). Introduction of excess alkali metal cations leads to a small downfield shift of both axial and equatorial resonances; the shift for axial ligand is significantly larger especially in the case of alkali metal cations (Table 4). As the ^{13}C NMR spectrum is a good measure of electron density on carbon atoms,[52–57] the results point to a noticeable decrease in electron density on the CN^- ligands as a result of interaction between cations and lone electron pairs localized on nitrogen atoms. The magnitude of these changes is not correlated directly with hydrated radii of cations, because the other important factors influencing these shifts are also acceptor properties of cations. The higher sensitivity of the axial NMR signal indicates that the *trans*-CN^- ligand is favoured in binding the hydrated alkali metal cation.

Table 4 Cation effect on the ^{13}C NMR shift for 0.5 M $Na_2[Fe(CN)_5NO]$ (cation concentrations up to 3 M) and ion pair equilibrium constants for some tetraalkylammonium cations

Cation	r_i^{∞} [a]/pm	h_i^{∞} [b]	$\Delta(\delta\ CN_{eq})$ [c]/ppm	$\Delta(\delta\ CN_{ax})$ [c]/ppm	K_{IP}
Na^+ counter ion			0	0	—
Li^+	307	7.4	0.23	0.40	—
Na^+	292	6.5	0.48	0.78	—
K^+	279	5.1	0.25	0.60	0.15
Rb^+	277	4.7	0.22	0.65	—
Cs^+	277	4.3	−0.14	0.21	—
$TRIS^+$ [d]	426 [e]	—	−0.43	−0.27	—
Bu_4N^+	396	0.0	−4.41	−4.52	0.45
Pr_4N^+	362	0.0	−3.29	−3.95	0.69
Et_4N^+	320	0.0	−2.18	−2.76	0.80
Me_4N^+	282	1.8	−1.42	−1.23	2.08
MV^{2+} [f]	200 [g], 560 [g] 330 [g], 600 [g]	—	−0.64	−0.58	—
$[K(18\text{-crown-}6)]^+$	480 [e]	—	−4.36	−4.41	—

[a] Hydrated radius of the cation.[58] [b] Hydration number.[58] [c] Chemical shift change with respect to an aqueous solution of nitroprusside. [d] Tris(hydroxymethyl)methylammonium. [e] Estimated using ArgusLab molecular dynamics software.[61] [f] *N*,*N*′-Dimethyl-4,4′-bipyridinium. [g] From ref. 29, for different possible molecular arrangements.

The behaviour of tetraalkylammonium cations is somewhat different and much simpler. They cannot interact directly with lone electron pairs localized at nitrogen atoms of CN^- ligands, they are weakly hydrated (or non-hydrated in most cases) and therefore their interaction is purely electrostatic. This is substantiated by a clear dependence of equilibrium constant on cation radius (Table 4), consistent with the ESIMS observations above, as well as previous studies in the nitroprusside–thiolate systems.[29–30] In contrast to alkali metal cations, they induce upfield shift of both axial and equatorial signals. This can be easily associated with a decrease of polarity in the environment of the nitroprusside anions: the same effect is observed when nitroprusside is dissolved in methanol.[51] The tetraalkylammonium cations [58] are usually not hydrated and their interaction with nitroprusside leads to partial dehydration of the complex anion, which results directly in the upfield shift of the carbon resonances. The largest shift (and hence the strongest dehydration of nitroprusside) is observed for tetrabutylammonium cation, as can be expected from the above model. In this case also axial ligands are more susceptible for interactions with cations.

Interaction with mercaptosuccinate

The addition of the potassium salt of mercaptosuccinic acid to $Na_2[Fe(CN)_5NO]$ results in the formation of several new species. As a result of the added potassium ion, the ion-pair $\{K^+[Fe(CN)_5NO]^{2-}\}^-$ at *m*/*z* 254.8 (calc. 255) appears in addition to the Na^+ and H^+ analogues, with intensity increasing with increasing ratio of potassium mercaptosuccinate to the Fe complex. More importantly, a range of better-defined but still relatively low intensity ion-paired mercaptosuccinate adduct complexes $\{M^+_x[Fe(CN)_5N(O)C_4H_{6-x}O_4S]^{2-}\}^-$ are observed as minor peaks at *m*/*z* 389.0, 405.0, 412.9, 554.8 (theor. 389, 405, 411, 555, respectively), with intensity increasing with an increase in concentration of mercaptosuccinate. This is consistent with the generation of *S*-nitrosothiolate complexes known to occur in the reversible general reaction [eqn. (1)]. Moreover, a low intensity ion-paired adduct containing two thiolate groups coordinated to the $[Fe(CN)_5NO]^{2-}$ complex is recorded at *m*/*z* 554.8 (theor. 555) (Table 5).

The adducts are usually thermally unstable, which would account for their existence as only minor species. Since the decomposition products from the thermal reaction are reduced nitroprusside and the disulfide—the former was found as $\{H^+_2[Fe^{I}(CN)_5NO]^{3-}\}^-$ at *m*/*z* 218.7 (theor. 218), whereas the latter should not be detected in ESIMS as a neutral species. However, in the present case we have employed a thiol with ionizable carboxylate groups present, and the observation of a peak at *m*/*z* 297.1 is consistent with the presence of the disulfide monoanion (theor. *m*/*z* 297). Notably, this peak increases substantially in size as the ratio of nitroprusside to mercaptosuccinate is increased from 1 : 1 to 1 : 10 {the total ion current for this signal increases from 0.04 (1 : 1), to 0.62 (1 : 2), 3.85 (1 : 5) and 7.97% (1 : 10) at a CV 10 V and 2×10^{-4} M nitroprusside}. Similar behaviour is shown by the disulfide radical monoanion signal at *m*/*z* 299.0. The signals provide indirect evidence of the intermediate through its catalysis of disulfide formation.[59] A further peak at *m*/*z* 148.7 shows a parallel concentration-dependent behaviour, and can be assigned as the disulfide dianion (theor. *m*/*z* 149). Importantly, the ESIMS of mercaptosuccinic acid in aqueous base at a CV 10 V but in the absence of nitroprusside shows clearly lower intensity peaks at *m*/*z* 297.1 and 148.7, which further defines the formation of the disulfide as catalysed by the nitroprusside. The mercaptosuccinate spectrum alone is dominated by the peak from the simple monoanion at *m*/*z* 148.7 (theor. *m*/*z* 149).

Conclusion

This study has established that the simple complex anion nitroprusside can be defined intact in the relatively 'soft' ESIMS experiment, and represents one of few studies of simple complex anions extant. In particular, data collection at low cone voltage provides for the best integrity of ions. Also most of the daughter ions are predictable fragments of the parent $[Fe(CN)_5NO]^{2-}$ anion (Table 1).

The specific cation effect on the nitroprusside reactivity has been more than once interpreted in terms of ion pair formation,[29–30,35,36] but previously no direct evidence was presented. Due to the enhancement of ion pair abundance by the ESI technique, the study provides this evidence for monovalent alkali metal (Table 2) and some alkylammonium cations (Table 3). The evidence is multiple: beside the $\{M^+[Fe(CN)_5NO]^{2-}\}^-$ anions, also $\{M_3[Fe(CN)_5NO]\}^+$ cations and more complex clusters of the type $\{M_x[Fe(CN)_5NO]_y\}^{z-/z+}$ were recorded. The trend in the ion pair formation seen in the ESIMS follows the series $Li^+ > Na^+ > K^+ > Rb^+ > Cs^+$ and $Me_4N^+ > Et_4N^+ > Pr_4N^+ > Bu_4N^+$ and is consistent with conception based on purely electrostatic arguments for unsolvated ions. The same argument is dominant in the bulk $[Fe(CN)_5NO]^{2-}$ solution; under these conditions, however, not naked but hydrated cation radii play the crucial role. Because of this, the series of cation activity in solutions only in the alkylammonium part resemble that found by the ESI technique, whereas activity

Table 5 ESIMS for 1×10^{-3} M $Na_2[Fe(CN)_5NO]$–mercaptosuccinic acid–KOH[a] solutions at pH 10 and a CV of 10 V

System studied	Species	m/z_{theor}	m/z_{obs}	%BPI
$C_4H_6O_4S$ + KOH	$C_4H_5O_4S^-$ or $(C_4H_5O_4S)_2^{2-}$	149	148.7	100
	$\{K^+(C_4H_4O_4S)^{2-}\}^-$	187	186.8	4.9
	$\{H^+(C_4H_4O_4S)_2^{2-}\}^-$	297	297.1	5.9
	$\{H^+(C_4H_5O_4S)_2^{2-}\}^-$	299	299.0	1.0
	$\{K^+(C_4H_4O_4S)_2^{2-}\}^-$	335	335.0	1.4
	$\{K^+(C_4H_5O_4S)_2^{2-}\}^-$	337	337.0	0.4
	$\{H^+(C_4H_6O_4S)\}^+$	151	150.8	0.4[b]
	$\{K^+(C_4H_6O_4S)\}^+$	189	188.9	0.4
	$\{K^+_2(C_4H_5O_4S)^-\}^+$	227	226.9	0.5
	$\{K^+_3(C_4H_4O_4S)^{2-}\}^+$	265	264.9	0.2
$C_4H_6O_4S$ + KOH + $Na_2[Fe(CN)_5NO]$ immediately after mixing	$\{H^+_2[Fe^{II}(CN)_5NO]^{3-}\}^-$	218	218.7	0.4[c]
	$\{K^+[Fe(CN)_5NO]^{2-}\}^-$	255	254.8	10
	$\{Na^+H^+_2[Fe(CN)_5NO(C_4H_6O_4S)]^{4-}\}^-$	389	389.0	0.1
	$\{K^+H^+_2[Fe(CN)_5NO(C_4H_6O_4S)]^{4-}\}^-$	405	405.0	0.25
	$\{Na^+_2H^+[Fe(CN)_5NO(C_4H_5O_4S)]^{4-}\}^-$	411	412.9	0.24
	$\{K^+_3[Fe(CN)_5NO(C_4H_4O_4S)]^{4-}\}^-$	481	481.3	0.06
	$\{K^+[Fe(CN)_5NO(C_4H_6O_4S)_2]^{2-}\}^-$	555	554.8	0.06
	$\{K^+Na^+(C_4H_5O_4S^-\}^+$	211	210.9	0.2[c]
	$\{K^+_3[Fe(CN)_5NO]^{2-}\}^+$ (s)	333	333.0	0.5
	$\{K^+_2Na^+[Fe(CN)_5NO]^{2-}\}^+$	317	317.0	0.1[c]
$C_4H_6O_4S$ + KOH + $Na_2[Fe(CN)_5NO]$ 24 h later	$\{H^+_2[Fe^{II}(CN)_5NO]^{3-}\}^-$	218	218.7	4.8[d]

[a] RSH : KOH = 1 : 3, $Na_2[Fe(CN)_5NO]$: RS^- = 1 : 5. [b] The signal intensity increases with the RSH : KOH ratio. [c] The signal intensity decreases with an increase in the K^+ : Na^+ ratio. [d] The signal characteristic of the Fe(II) complex increases significantly within 24 h at the expense of all signals recorded immediately after mixing $[Fe(CN)_5NO]^{2-}$ and mercaptosuccinate, except for those signed (s) or described in footnote (b).

of alkali metal cations proceeds conversely, *i.e.* $Li^+ < Na^+ < K^+ < Rb^+ < Cs^+$.[29–30] The series was verified by the ^{13}C NMR spectra, which point to CN^- in the axial position as especially susceptible to binding one of these cations (Table 4).

The ESI results clearly document the cation role in mediating the reaction between nitroprusside and anions. Moreover, short-lived adducts with thiolates of the type $\{M^+_3[Fe(CN)_5NO(C_4H_4O_4S)]^{4-}\}^-$ have been defined by their observation directly and through their decomposition products (Table 5), providing further support for reversible nitrosothiol complex formation [eqn. (1)]. The equilibrium between nitroprusside with thiolates and the nitrosothiol adducts has been shown to be significantly influenced by the concentration and nature of the cations employed. This has been thought to be associated with cation–anion ion pairing, since small cations promote nitrosothiol complex formation, whereas large cations retard the reaction. Moreover, the cations influence the $[Fe(CN)_5N(O)SR]^{(n+2)-}$ complex stability that confirms the previous observation.[29]

Given that the nitrosothiol complex must be formed by the reaction of two anionic species, charge reduction of the complex component of the reactants through tight ion pairing is anticipated to be the source of the effect. Moreover, mercaptosuccinate is also able to form ion pairs with cations (Table 5) making the formation of the nitrosothiol complex even easier. The observation here of clear cation size-dependent ion pairing between the nitroprusside and added cations supports this argument. Notably, however, we find that even bulky alkylammonium ions show evidence of some ion pairing (Table 3) since the ESI technique enhances ion pair concentrations. In this way, it can be employed to probe and infer the existence of even weak ion pairing in bulk solutions.

This enabled us presumably to detect also the dinitrosothiol complex in the form of the ion pair with potassium cation, $\{K^+[Fe(CN)_5NO(C_4H_6O_4S)_2]^{2-}\}^-$ and the disulfide anion radical (Table 5). These two unstable species were recently suggested to be intermediates in the spontaneous and autocatalyzed redox decomposition of the $[Fe(CN)_5N(O)SR]^{(n+2)-}$ complex, where H_nRS = cysteine, *N*-acetylcysteine, ethyl cysteinate and glutathione.[59]

The present study has shown how the ESIMS technique can provide information relevant to both thermodynamic and kinetic processes in coordination chemistry even where species of limited stability are involved.

Experimental

Chemicals and instrumentation

Sodium nitroprusside (Merck), glutathione (Aldrich), mercaptosuccinic acid and other chemicals of the highest available purity were used as purchased. Sample solutions were prepared by dissolving solid samples in deionized water to produce stock solutions, from which required solutions were prepared by mixing measured volumes of the reagents as desired and diluting to a known volume and concentration. The concentration of all sample solutions was between 1×10^{-4} and 1×10^{-3} M, with most studies employing typically 2×10^{-4} M solutions. For investigation of selective cation ion pairing of sodium nitroprusside with other cations, aqueous solutions of this complex with the cations in equimolar or selected higher concentrations were prepared. All analyte samples (in 1.8 mL vials) were readily introduced using an auto injector, which was rinsed thoroughly with solvent between injections.

All the ESIMS experiments were performed on a VG Platform II single quadrupole mass spectrometer (Micromass Ltd., Altrincham, UK) coupled to a HPLC binary pump system. For all spectral acquisitions, the tip of the capillary was at a potential of ±3.5 kV relative to ground. The source temperature was maintained at 80 °C, and nitrogen was used as the bath and nebulizing gas. The mobile phase solution was the same as the solvent of the analyte solution. An optimum flow rate of 10 μL min^{-1} was employed. A Reodyne injector fitted with a 10 μL loop was used to inject the sample solution into the flow of the mobile phase. The cone voltage (CV) was varied between +10 to +60 for positive-ion and −10 to −50 V for negative-ion mode. For most studies, the lowest CV was employed.

Mass spectra were acquired by scanning the quadrupole mass filter from *m/z* 2000 to 2, and ions were detected by means of a scintillator detector. Approximately 40 scans were summed to give a mass spectrum. All data were acquired and processed using the Micromass MassLynx system. Experimental peak values throughout this study are identified by the *m/z* ratio of the most abundant peak in the parent group. Calculated *m/z* values tabulated are those based on the most abundant isotopes. Observed peak intensities are usually cited as percentages of the base (major) peak intensity (%BPI). Where relative abundances are reported in tables, these have been obtained by adjusting for ion efficiency by calibration against the corre-

sponding equimolar $Li^+/Na^+/K^+/Rb^+/Cs^+$ or $Me_4N^+/Et_4N^+/Pr_4N^+/Bu_4N^+$ free ion spectra, recorded for separate mixtures of these two families of ions at the common cone voltage of 10 V.

^{13}C NMR spectra were recorded on a Bruker AC200 spectrometer in water; $(CH_3)_4Si$ in C_6D_6 in coaxial tube was used as an external standard. It was assumed that cation exchange in ion pairs is fast on the NMR timescale and the observed chemical shift is the weighted mean of the chemical shifts of the signals due to free nitroprusside (NP) and the ion pair (IP):[60]

$$\delta = \frac{\delta_{NP}[NP] + \delta_{IP}[IP]}{[NP] + [IP]} \quad (3)$$

Combination of eqn. (3) with the expression for the equilibrium constant for ion pair formation, eqn. (4),

$$K_{IP} = \frac{[IP]}{[NP][M^+]} \quad (4)$$

allows estimation of K_{IP} provided that ^{13}C NMR spectra are recorded for at least two different concentrations of cations:

$$K_{IP} = \frac{\delta_{NP}M_1 + \delta_1 M_2 - \delta_2 M_1}{2M_1M_2(\delta_2 - \delta_1)} \quad (5)$$

where δ_{NP} denotes the chemical shift of pure nitroprusside, δ_1 and δ_2 are the chemical shifts in the presence of cation at concentrations M_1 and M_2, respectively. Results obtained for axial and equatorial signals are within the same experimental error.

Acknowledgements

We are grateful to the University of Newcastle for financial support of Z. S. under a Research Visitor Scheme. The technical assistance of Mark Graham in the collection of ESIMS is acknowledged and greatly appreciated.

References

1 P. Chen and T. J. Meyer, *Chem. Rev.*, 1998, **98**, 1439.
2 P. D. Metelski and T. W. Swaddle, *Inorg. Chem.*, 1999, **38**, 301.
3 Y. Fu and T. W. Swaddle, *Inorg. Chem.*, 1999, **38**, 876.
4 A. Zahl, R. van Eldik and T. W. Swaddle, *Inorg. Chem.*, 2002, **41**, 757.
5 T. Vilariño, P. Alonso, L. Armesto, P. Rodríguez and M. E. Sastre de Vicente, *J. Chem. Res. (S)*, 1998, 558.
6 D. A. Estrin, L. M. Baraldo, L. D. Slep, B. C. Barja, J. A. Olabe, L. Paglieri and G. Corongiu, *Inorg. Chem.*, 1996, **35**, 3897.
7 G. C. Pedrosa, N. L. Hernandez, N. E. Katz and M. Katz, *J. Chem. Soc., Dalton Trans.*, 1980, 2297.
8 M. del Mar Graciani, M. A. Rodriguez and M. L. Moya, *Int. J. Chem. Kinet.*, 1997, **29**, 377.
9 M. A. Blesa, E. B. Borghi and R. Fernandez-Prini, *J. Chem. Soc., Faraday Trans. I*, 1985, **81**, 3021.
10 S. Alshehri, J. Burgess, G. H. Morgan, B. Patel and M. S. Patel, *Transition Met. Chem.*, 1993, **18**, 619.
11 R. E. Shepherd, M. F. Hoq, N. Hoblach and C. R. Johnson, *Inorg. Chem.*, 1984, **23**, 3249.
12 L. W. Warner, M. F. Hoq, T. K. Myser, W. W. Henderson and R. E. Shepherd, *Inorg. Chem.*, 1986, **25**, 1911.
13 M. K. Basu and M. N. Das, *Inorg. Chem.*, 1970, **9**, 2781.
14 D. W. Larsen and A. C. Wahl, *Inorg. Chem.*, 1965, **4**, 1281.
15 Y. I. Rutkovskii and V. E. Mironov, *Russ. J. Inorg. Chem.*, 1967, **12**, 1739.
16 P. Bindra, H. Gerischer and L. M. Peter, *Electroanal. Chem. Interfacial Electrochem.*, 1974, **57**, 435.
17 D. Krulic, N. Fatouros and D. E. Khoshtariya, *J. Chim. Phys.*, 1998, **95**, 497.
18 L. M. Peter, W. Dürr, P. Bindra and H. Gerischer, *J. Electroanal. Chem.*, 1976, **71**, 31.
19 M. Das-Sharma, S. Gangopadhyay, M. Ali and P. Banerjee, *J. Chem. Res. (S)*, 1993, 122.
20 P. C. Ford, J. Bourassa, K. Miranda, B. Lee, I. Lorkovic, S. Boggs, S. Kudo and L. Laverman, *Coord. Chem. Rev.*, 1998, **171**, 185.
21 G. Stochel, A. Wanat, E. Kuliś and Z. Stasicka, *Coord. Chem. Rev.*, 1998, **171**, 203.
22 K. Szaciłowski, W. Macyk, G. Stochel, Z. Stasicka, S. Sostero and O. Traverso, *Coord. Chem. Rev.*, 2000, **208**, 277.
23 J. L. Bourassa and P. C. Ford, *Coord. Chem. Rev.*, 2000, **200**, 887.
24 D. J. Sexton, A. Muruganandam, D. McKenney and B. Mutus, *Photochem. Photobiol.*, 1994, **59**, 463.
25 V. R. Zhelyaskov, K. R. Gee and D. W. Goldwin, *Photochem. Photobiol.*, 1998, **67**, 282.
26 K. Szaciłowski and Z. Stasicka, *Prog. React. Kinet. Mech.*, 2000, **26**, 1.
27 M. D. Johnson and R. G. Wilkins, *Inorg. Chem.*, 1984, **23**, 231.
28 A. R. Butler and C. Glidewell, *Chem. Soc. Rev.*, 1987, **16**, 361.
29 K. Szaciłowski, G. Stochel, Z. Stasicka and H. Kisch, *New J. Chem.*, 1997, **21**, 893.
30 O. R. Leeuwenkamp, C. H. Vermaat, C. M. Plug and A. Bult, *Pharm. Weekbl.*, 1984, **6**, 195.
31 A. R. Butler, A. M. Calsy and I. L. Johnson, *Polyhedron*, 1990, **9**, 913.
32 D. Tsikas, R. H. Böger, S. M. Bode-Böger, G. Brunner and J. Frölich, *J. Chromatogr., A*, 1995, **699**, 363.
33 J. Reglinski, A. R. Butler and C. Glidewell, *Appl. Organomet. Chem.*, 1994, **8**, 25.
34 S. Aleryani, E. Milo and P. Kostka, *Biochim. Biophys. Acta*, 1999, **1472**, 181.
35 K. Szaciłowski, J. Oszajca, A. Barbieri, A. Karocki, Z. Sojka, S. Sostero, R. Boaretto and Z. Stasicka, *J. Photochem. Photobiol., A: Chem.*, 2001, **143**, 99.
36 K. Szaciłowski and Z. Stasicka, *Coord. Chem. Rev.*, 2002, **229**, 17.
37 D. K. Walanda, R. C. Burns, G. A. Lawrance and E. I. Von Nagy-Felsobuki, *J. Chem. Soc., Dalton Trans.*, 1999, 311.
38 R. Colton, A. D'Agostino and J. C. Traeger, *Mass Spectrom. Rev.*, 1995, **14**, 79.
39 J. C. Traeger, *Int. J. Mass Spectrom.*, 2000, **200**, 387.
40 G. A. Lawrance, M. J. Robertson, E. I. Sutrisno and Von Nagy-Felsobuki, *Inorg. Chim. Acta*, 2002, **328**, 159.
41 E. I. Sutrisno, Y. Baran, G. A. Lawrance, E. I. Von Nagy-Felsobuki, D. C. Richens and H. Xiao, *Inorg. Chem. Commun.*, 1999, **2**, 107.
42 D. K. Walanda, R. C. Burns, G. A. Lawrance and E. I. Von Nagy-Felsobuki, *J. Cluster Sci.*, 2000, **11**, 5 and references therein.
43 J. M. Slocik, K. V. Somayajula and R. E. Shepherd, *Inorg. Chim. Acta*, 2001, **320**, 148.
44 G. Wolfbauer, A. M. Bond and D. R. McFarlane, *J. Chem. Soc., Dalton Trans.*, 1999, 4363.
45 G. Wolfbauer, A. M. Bond and D. R. McFarlane, *Inorg. Chem.*, 1999, **38**, 3836.
46 R. K. Upmacis, P. D. Hajjar, B. T. Chait and U. A. Mizra, *J. Am. Chem. Soc.*, 1997, **119**, 10424.
47 M. Lewin, K. Fischer and I. G. Dance, *Chem. Commun.*, 2000, 947.
48 J. M. Slocik, M. S. Ward, K. V. Somayajula and R. E. Shepherd, *Transition Met. Chem.*, 2001, **26**, 351.
49 S. Chand, R. K. Coll and J. S. McIndoe, *Polyhedron*, 1998, **17**, 507.
50 H. Wang and G. R. Agnes, *Anal. Chem.*, 1999, **71**, 4166.
51 A. R. Butler, C. Glidewell, A. S. McIntosh, D. Reed and I. H. Sadler, *Inorg. Chem.*, 1986, **25**, 970.
52 J. M. Malin, C. F. Schmidt and H. E. Toma, *Inorg. Chem.*, 1975, **14**, 2924.
53 W. P. Griffith, M. J. Mockford and A. C. Skapski, *Inorg. Chim. Acta*, 1987, **126**, 179.
54 B. A. Narayanan and P. T. Manoharan, *J. Inorg. Nucl. Chem.*, 1978, **40**, 1993.
55 A. D. James and R. S. Murray, *Inorg. Nucl. Chem .Lett.*, 1976, **12**, 739.
56 H. E. Toma and J. A. Vanin, *Inorg. Chim. Acta*, 1979, **33**, L157.
57 A. R. Butler, C. Glidewell, A. R. Hyde and J. McGinnis, *Inorg. Chem.*, 1985, **24**, 2931.
58 Y. Marcus, *Ion Solvation*, J. Wiley & Sons Ltd., New York, 1985.
59 K. Szaciłowski, A. Wanat, A. Barbieri, E. Wasielewska, M. Witko, G. Stochel and Z. Stasicka, *New J. Chem.*, 2002, **26**, in press.
60 V. A. Grigoriev, D. Cheng, C. L. Hill and I. A. Weinstock, *J. Am. Chem. Soc.*, 2001, **123**, 5292.
61 ArgusLab 2.0.0., Planaria Software 1996–2001, available at http://www.planaria-software.com.